NAMDEV A. PATIL[1*], SRINIVASA RAO PEDAPATI[1], OTHMAN BIN MAMAT[1]

A REVIEW ON ALUMINIUM HYBRID SURFACE COMPOSITE FABRICATION USING FRICTION STIR PROCESSING

Nowadays, Aluminium (Al) based hybrid surface composites are amongst the fastest developing advanced materials used for structural applications. Friction Stir Processing (FSP) has emerged as a clean and flexible solid-state surface composites fabrication technique. Intensive research in this field resulted in numerous research output; which hinders in finding relevant meta-data for further research with objectivity. In order to facilitate this research need, present article summarizes current state of the art and advances in aluminium based hybrid surface composites fabrication by FSP with in-situ and ex-situ approach. Reported literature were read and systematically categorized to show impacts of different types of reinforcements, deposition techniques, hybrid reinforcement ratio and FSP machine parameters on microstructures, mechanical and tribological characteristics of different Al alloys. Challenges and opportunities in this field have been summarized at the end, which will be beneficial to researchers working on solid state FSP technique.

Keywords: Friction Stir Processing, Aluminium Hybrid Surface Composites, Mechanical Properties, Tribological Properties

1. Introduction

Abundantly available aluminium and its alloys are important materials preferred in various structural applications in automotive, light rail, marine, aerospace, etc. industries mainly because of their high specific strength, light weight, high ductility and good corrosion resistance [1]. The design engineers are looking for light weight and high strength materials for structural applications. Aluminum alloys are replacing steel alloys in various applications due to their high specific strength and low density [2-4]. However, poor surface properties like wear resistance under high load applications are restricting their wider applications. Unlike steels, Al alloys can't be hardened significantly by induction hardening since martensitic phase is not available. Thin hard coatings do not sustain on Al alloys in high loading applications due to 'thin-ice effect' [5]. So rigorous scientific research to improve their material properties gave rise to various effective alternative methods. Amongst these methods, fabrication of bulk and surface Metal Matrix Composites (MMC) has become most popular from more than last three decades. Important potential of MMC approach is ability to induce customized properties with help of introducing particular reinforcements [6]. For many engineering applications

spectrum of material properties required are broad enough so that those cannot be full filled using single reinforcement. Thus deposition of two or more reinforcements into metal alloy has become essential and is known as metal matrix hybrid composites approach. This approach has generated many opportunities in developing low cost-high performance material with possibilities of tailoring their customized properties [7]. Al based mono and hybrid MMCs have shown high specific strength, high specific modulus, improved fatigue, improved resistance to corrosion and wear. Such ability to induce customized properties have made mono and hybrid MMCs famous in materials research field [7-8].

In surface engineering field, surface MMCs have been synthesized through various methods like plasma spraying [9], cold spraying [10], laser melting [11-14], cast sinter [15-16] and electron beam irradiation method [17] etc. These fabrication techniques have many disadvantages such as particle agglomeration, formation of detrimental phases and interfacial reactions because of processing above melting point temperatures of respective metal alloys. Then disadvantages of these above mentioned techniques highlighted a need to find effective alternative method for synthesis of MMCs. In 1999, R.S. Mishra et al. proposed FSP technique, in which intense plastic deformation has been used to induce superplasticity in Al 7075 alloy successfully [18]. After-

[1] DEPARTMENT OF MECHANICAL ENGINEERING, UNIVERSITI TEKNOLOGI PETRONAS, MALAYSIA

* Corresponding author: namdev_17003401@utp.edu.my
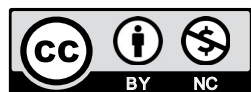
wards they have fabricated the Al-silicon carbide (SiC) ex-situ surface composites using same FSP technique [19]. Then this novel, solid state processed and eco-friendly technique became more popular amongst the researchers and led to numerous researches on surface composites fabrication using FSP.

FSP technique is based on principle of friction stir welding (FSW); which is invented by TWI, Cambridge, UK in 1991 [20]. In FSP, material is subjected to intense plastic deformation due to thermo-mechanical friction stirring action. It comprises both heat generation due to friction and material flow due to continuous stirring action of the tool. In this, the rotating FSP tool is plunged into workpiece and traverses, during which plasticized material reaches to temperature less than melting point temperature of the material [21-26]. The composite fabrication using FSP involves both in-situ and ex-situ approach, and this process is complex because it involves many process parameters. The responses in terms of various material properties of the base alloys are observed to be different in nature to one another for the same set of process parameters used. Also to replicate the desired material properties at various processing systems with respect to some chosen process parameters, it is necessary to have good control over the work environment. The Al alloys shows changed responses for comparable process parameters merely due to their different nature of metallurgical and structural behavior and thus it becomes essential to know the response of each alloy type to the respective processing conditions thoroughly. Thus for this purpose, there is need to present state of the art in a systematic manner to the researchers in this field. This article is written with focus on fabrication process of hybrid Al surface MMCs using FSP on various aluminum alloys. Also the effects of various types of reinforcements and involved FSP process parameters on microstructure, mechanical and tribological properties of base Al alloys used in the process.

2. Fabrication of Al alloy based Hybrid Surface Composites using FSP

FSP technique is utilized to develop Al hybrid composites through mainly two approaches- by in-situ and ex-situ approach. In in-situ approach, the required reinforcement phases have to be developed during processing by reactions of deposited precursor mixture with the base alloy. Whereas in ex-situ route, already developed reinforcements are directly embedded during processing in to the base alloy. Fabrication of composites using in-situ approach facilitates much clean interfaces between reinforcements and base alloy substrate. In-situ approach gives better dispersion of reinforcements without impurities since reaction happens in a controlled environment inside stir zone. However, in-situ approach has less options of reinforcements and combinations [27]. The ex-situ approach facilitates more number of reinforcement combination options. In ex-situ route the care must be taken about purity of the reinforcements and cleanliness of the deposition locations on the base alloy [28]. The fabrication of hybrid surface composites by both in-situ and ex-situ approach

involves many process parameters. One of the parameters is the strategy of pre-placing the particle of reinforcement over the base plate and then embedding it via FSP. From time to time, researchers have used multiple methods to pre-place reinforcements on substrates, including pre-placed particle layers, through grooves, through surface blind holes and some have used cold spraying methods, mechanical alloy methods, multichamber method, and direct friction stir processing (DFSP) methods.

Generally preplaced reinforcements are packed into the substratum by running with a pinless shoulder tool or by using a thin Al foil before the final FSP to originally cover the particles filled grooves or holes to avoid sputtering. Interestingly, in multichamber technique [29], the surface blind holes are processed by avoiding the particle sputtering using single tool by performing FSP in two steps. In the DFSP method, there is facility of simultaneous reinforcement's addition through tool itself while performing FSP [30]. From the studies summarized it's clear that Al alloys behaves very differently to comparable processing conditions merely because of the different nature of its metallurgical, structural behavior and thus it becomes essential to know the response of each alloy type to the respective processing conditions thoroughly.

2.1. Hybrid reinforced wrought aluminium composites

2.1.1. 1xxx series

The Al 1xxx alloy group consists of super-pure and different commercially-pure grades of aluminium alloys. From initial phase of industry, these alloys have been used in wrought product forms for many applications including chemical process equipments, electrical conductors, foils etc. These materials have high electrical conductivity, formability and corrosion resistance. The tensile strength of these alloy ranges between 45-165 MPa [31]. However these alloys can only be strengthened more by using cold working as they are non-heat treatable alloys. The summary of Al 1xxx based hybrid surface composites fabrication is given in Table 1.

Using functionality of FSP and addition of reinforcements, the mechanical and tribological properties of these alloys were improved by means of activating different strengthening mechanisms. In order to activate distinct strengthening routes, grain size refinement was noted primarily owing to dynamic recrystallization using intense FSP plasticization and grain growth pinning through the incorporation of hard particles. Mainly strengthening due to load transfer mechanism with good interfacial bonding, Orowan mechanism, grain refinement – Hall Petch relationship, coefficient of thermal expansion mismatch, elastic modulus mismatch and increase in dislocation density were observed by researchers. The variations in the microhardness and ultimate tensile strength of Al 1xxx based hybrid surface composites is as shown in Fig. 1 and Fig. 2 respectively.

Dixit et al. [37] found that interfacial bonding between aluminium and graphene was continuous, due to which dislocations

TABLE 1

A Summary of hybrid surface composites fabrication on Al 1xxx alloys

Base Material and size	Reinforcement and Preplacement Method	Tool Material and Specifications	FSP Process Parameters	Prominent Results	Reference
Al 1050 L – 210 mm, W – 70 mm, T – 5 mm.	Fe_2O_3 (1 μm), Al (100 μm), milled for 1, 2 and 3 – h, Groove Method: GD – 3.5 mm, GW – 1.4 mm.	H – 13 steel tool: Straight cylindrical threaded pin, SD – 18 mm, PD – 5 mm, PL – 4 mm, Threads depth – 0.5 mm with angle 30°.	Capping pass: w – 1120 rpm, ν – 125 mm/min. FSP pass: w – 1400 rpm and ν – 40 mm/min.	The ultimate tensile strength (UTS) of the hybrid nano composite was a function of milled time for reinforcements. Hybrid composites showed significant increase in tensile strength (97 to 159 MPa) and hardness (33 to 75 HV) than base alloy.	Ghasem Azimi – Roeen et al. 2017 [32]
Pure Aluminium 150 mm×50 mm×6 mm.	SiC (3.6 μm) and Gr used for synthesizing Graphene Oxide (GO) decorated SiC, Surface Blind Holes Method: ɸ – 2 mm, depth – 4 mm, inter – cavity spacing – 3 mm.	D2 die steel tool: concave shoulder, threaded cylindrical pin, SD – 18 mm, PD – 6 mm, PL – 5.5 mm.	FSP Pass: w – 600 rpm, ν – 20 mm/min, TT – 1°, F – 10 KN, No. of pass – 1.	The UTS of Al/GO (graphene oxide) encapsulated SiC hybrid composite was higher than pristine Al, Al/SiC composite by the factor of nearly 3.4 and 1.3 respectively. They observed that Al/ GO (graphene oxide) encapsulated SiC hybrid composite had 98% increase in storage modulus.	Subhash Singh et al. 2017 [33]
Al – 1050 L – 130 mm, W – 60 mm, T – 5 mm.	Al (50 μm), TiO_2 (10 μm) and graphite (10 μm), used with 1. As mixed, 2. 60 h ball milled condition. Groove Method GW – 1 mm, GD – 3 mm.	Concave Shoulder surface, Straight cylindrical pin, SD – 18 mm, PD – 5 mm, PL – 4.8 mm.	FSP Pass: w – 950 rpm, ν – 37.5 mm/min, No. of passes – 4 with changing AS to RS in each pass.	They found higher hardness and UTS (110 MPa) due to TiC (100nm) produced in – situ for hybrid composites ball – milled mixture than that of as – mixed mixture.	R. Beygi et al. 2016 [34]
Al 1050 L – 210 mm, W – 70 mm, T – 5 mm.	Fe_2O_3 (1 μm), Al(100 μm), milled for 1, 2, 3h Groove Method: GD – 3.5 mm GW – 1.4 mm.	H13 steel tool SD – 18 mm, PD – 5 mm, PL – 4 mm, threads of 0.5 mm depth and 30° angle.	Capping Pass: w – 1120 rpm, ν – 125 mm min – 1, FSP Pass: w – 1400 rpm and ν – 40 mm min – 1, No. of passes – 4.	High angle grain boundaries increased during FSP due to dynamic restoration phenomenon in processed zone. The grain size had decreased more when the powder milled for more time was encapsulated. The reactive powders addition had helped in increasing low ΣCSL boundaries.	Ghasem Azimi Roeen et al. 2017 [35]
Al 1050 – H24 T – 5 mm.	SiC (1.25 μm), Al_2O_3 (1.25 μm), Groove Method: GW – 3 mm, GD – 1.5 mm.	SKD61 steel tool SD – 14 mm a square probe diagonal length – 5 mm, PL – 3.3 mm.	w – 1500 rpm, ν – 1.66 mm/s TT – 3°, No. of FSP passes – 3 with changing AS to RS in each pass.	Higher microhardness was reported for mono SiC composite. They found that for load of 5 N the (SiC 80%, Al_2O_3 20%) combined hybrid composite shown excellent wear resistance than other hybrid ratios.	E.R.I. Mahmoud et.al. 2010 [36]
Pure aluminium plate T – 6 mm.	Gr (40 atomic %), Al (60 atomic %) Groove Method: GW – 3 mm, GD – 4 mm, Sealed with thin Al foil.	Plain tapered cylindrical pin in capping, with spiral grooves in FSP, PD – 6 mm at the bottom; 8 mm on the top.	No. of passes – 8.	Exfoliation of graphite to graphene took place successfully. Hardness increases from 31.6 ±0.4 HV to 48.7 ± 0.6 HV in the composite compared to base plate. The improved UTS – 147 MPa and 33% ductility attained by the composite due to good bonding between graphene and pure aluminium.	Dixit et.al. (2017) [37]

Note: UTS – Ultimate Tensile Strength , HV – Microhardness Value, L – length, W – width, T – Thickness, w – tool rotational speed, ν – tool traverse speed, AS – Advancing Side, RS – Retreating Side, SD – Shoulder Diameter, PD – pin diameter, PL – Pin length, TT – tool tilt angle, F – Axial force, GD – groove depth, GW – groove width, ɸ – hole diameter, FSPed – Friction Stir Processed, FSP – friction stir processing, MMC – Metal matrix composite.

motion were restricted in the Al-graphene nano composites. The micron size graphite exfoliated up to 6 μm thickness multilayer graphene sheets were homogenously distributed using multi pass FSP (8 passes). They found that presence of well bonded multi-layer graphene with metal matrix enhanced strength and ductility. Singh et al. [26] pointed out that MMCs functionality and mechanical properties were governed by controlling the problem of de-agglomeration, grain size of composites and surface morphology and distribution of dispersoids. They produced Al-SiC/graphene oxide (GO) composites without intermetallic

compounds and thus improved dispersibility and stability of dispersoids. Agglomeration of SiC particles significantly diminished by GO (graphene oxide) decoration. Using dynamic recrystallization during FSP, equiaxed fine grain structures were obtained from the elongated grains in as cast pristine Al matrix. Such that average grain size reduced from 160 μm to 4 μm in the resultant hybrid nano composite. They mentioned that GO (graphene oxide) helped in enhancing the interfacial bonding in Al-SiC/GO (graphene oxide) composite. This increased bonding at the matrix and dispersoids interfaces was mainly responsible for enhanced storage modulus and strength in resultant material.

Beygi et al. [34] and Azimi-Roeen et al. [32] both emphasized that ball milling of hybrid mixture prior to FSP not only enhanced reaction rates inside the stir zone by energizing the particles but also refined particles sizes. Beygi et al. [34] found that titanium oxide (TiO$_2$) (10 μm) and graphite (Gr) (10 μm) particles were broken into finer sizes due to ball milling and thus titanium carbide (TiC) (100 nm) particles were induced as a reaction product in the stir zone after FSP. The mixture without ball milling couldn't produce TiC phase after FSP, since friction stirring was not able to break graphite particles into finer ones. Therefore graphite particles didn't dissolve in Al matrix to form Al$_4$C$_3$. The microhardness values were homogenous across the
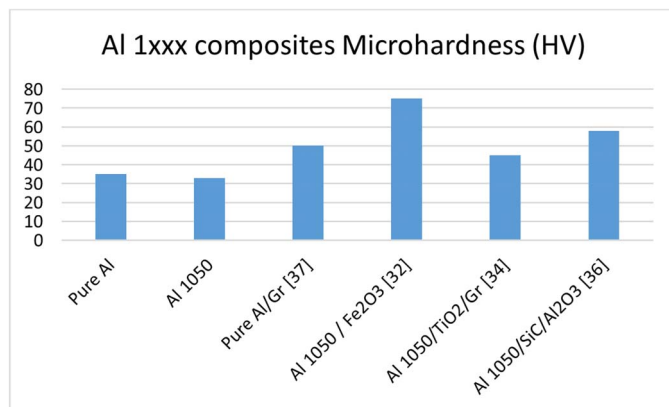

Fig. 1. Microhardness (HV) values of Al 1xxx series hybrid surface composites

Fig. 2. Ultimate tensile strengths of Al 1xxx series hybrid surface composites

stir zone of hybrid composite resulted due to homogenous particle distribution. The improved strength of Al 1050-TiC-Al$_3$Ti hybrid composites was attributed to Orowan strengthening. Particles refinement and their dispersion promoted due to high strain rate plastic deformation during FSP. Azimi-Roeen et al. [32] found that load transfer due to good interfacial bonding and grain refinement by Hall Petch relation were prominent strengthening mechanisms in Al 1050-(Al$_{13}$Fe$_4$+Al$_2$O$_3$) hybrid composites. The average grain size inside hybrid composites were 3.2 μm, 3.1 μm and 2.1 μm after FSP with ball milled (Fe$_2$O$_3$+Al) powders for 1 h, 2 h and 3 h respectively. The base alloy average grain size was 7.8 μm. The intermetallic compounds like Al$_{13}$Fe$_4$, Al$_2$O$_3$ and Fe$_3$O$_4$ acted as nucleation sites for resisting grain growth in the composites.

Mahmoud et al. [36] fabricated Al 1050/SiC/ Al$_2$O$_3$ hybrid surface composites with ex-situ approach and studied their mechanical and wear properties. They used multipass FSP and obtained uniform dispersal of the reinforcements. The Al$_2$O$_3$ particles surrounded by some minuet voids were reported in the microstructural observations. They reported that inclusion of hard SiC particles helped in improving the hardness of composite layer. However after introducing Al$_2$O$_3$ particles hardness get decreased. The higher microhardness was reported for mono Al 1050/SiC composite. The wear properties showed variations depending on the hybrid ratio of reinforcements and the load used during testing. They found that (SiC 80%, Al$_2$O$_3$ 20%) combined hybrid composite have shown excellent wear resistance than other composites with another hybrid ratios. They found that increasing the load in wear testing beyond certain critical value may change the wear mechanism from mild wear to severe wear and this value is vital as far as anti-wear material design concerned. They noted that Al$_2$O$_3$ had contributed in such a way that wear resistance increased and coefficient of friction decreased with its increased content in the hybrid mixture with SiC.

In terms of hybrid ratio optimization as an important variable, Dixit et al. [37] recommended that lubricative graphite powder should be added with other non-lubricative metallic or non-metallic powder in order to avoid tattering of FSP band due to high thermal conductivity and to achieve proper consolidation. The optimum hybrid ratio of powders used was (40atomic%Gr+60atomic%Al) for getting defect free FSP bands. Mahmoud et al. [36] found (80%SiC+20% Al$_2$O$_3$) as optimum hybrid ratio for highest wear resistance.

For FSP of Al 1xxx hybrid composites, tool rotational speeds reported were from 600 rpm to 1500 rpm. The tool traverse speeds used were between 20 mm/min to 100 mm/min. The number of passes reported were 3 to 8 in multipass FSP methods by various researchers. The multiple passes with 100% overlapping in same traverse direction and with change of traverse direction were reported useful. The tool materials used in FSP of this series were H13 steel [32,35-36] and D2 die steel [33]. The pin probe shapes like threaded straight cylindrical [32-33], square [36] and conical threaded [37] were used.

By in-situ approach, micron sized ball milled Fe$_2$O$_3$+Al, TiO$_2$+Al+Gr mixtures were deposited into the base alloys us-

ing groove method in order to produce $Al_2O_3+Al_{13}Fe_4$, TiC as reinforcement phases. By ex-situ approach, $(SiC+Al_2O_3)$ and (Al+Gr) mixtures were deposited using groove method. The GO (graphene oxide) coated SiC particles were deposited into the base alloy using surface blind holes method. Amongst them Al-SiC/GO (graphene oxide) hybrid composite produced by surface blind holes method gave higher strength and ductility compared to other composites.
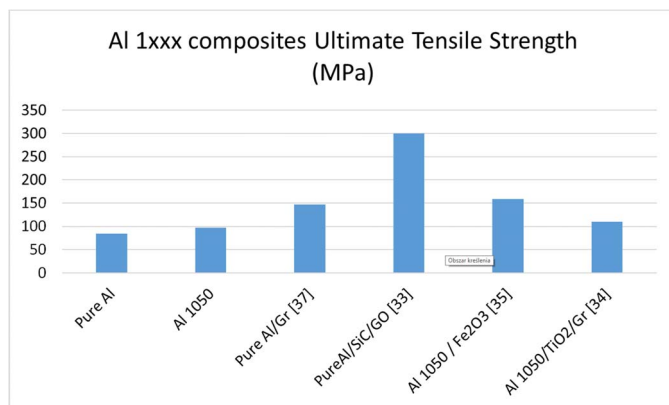
Thus for Al 1xxx series hybrid surface composites, the GO (graphene oxide) decorated SiC helped in achieving maximum tensile strength as compared to other combinations. The multiple passes strategy was majorly used by many researchers for Al 1xxx hybrid composites. The optimum FSP machine parameters used for successful fabrication of composites are enlisted in Table 2. The microhardness, tensile strength, ductility, fracture toughness, hot deformability and wear resistance were improved using the FSP characteristics along with reinforcements inherited properties.

2.1.2. 5xxx series alloys

The Al 5xxx group represents non heat treatable, strain hardenable alloys with Mg as main alloying element. The materials have been utilized for cryogenic pressure vessels, superstructures in ship vessels, bulk tanks for domestic milk/petrol transportation, parts of military vehicles such as ballistic armor plates and hulls of small boats. These alloys have good toughness, weldability and corrosion resistance. The tensile strength of range 40 MPa-310 MPa can be obtained with various grades of this series [31,38]. The Table 3 summarizes state of the art for fabrication of Al 5xxx based hybrid composites using FSP.

Researchers utilized FSP technique to incorporate effective reinforcements into the Al 5xxx series alloys substrates and succeeded in improving mechanical and tribological properties. The microhardness and ultimate tensile strength of Al 5xxx based hybrid surface composites are compared in Fig. 3 and Fig. 4 respectively. Sahandi et al. [44] found that strength of the

TABLE 2

Successful FSP machine parameters used for Al 1xxx hybrid surface composites

Composite	Tool rotational speed (w)	Tool traverse speed (v)	No. of passes	Reference
Al 1050/ Fe_2O_3	1400 rpm	40 mm/min	P-4	Azimi-Roeen et al. 2017 [32]
Pure Al/ SiC/GO (graphene oxide)	600 rpm	20 mm/min	P-1	Singh et al. 2017 [33]
Al 1050/TiO_2/Gr	950 rpm	37.5 mm/min	P-4	R. Beygi et al. 2016 [34]
Al 1050-H24/SiC/Al_2O_3	1500 rpm	1.66 mm/s	P-3	Mahmoud et.al. 2010 [36]

TABLE 3

A Summary of hybrid surface composites fabrication on Al 5xxx alloys

Base Material and size	Reinforcement and Preplacement Method	Tool Material and Specifications	FSP Process Parameters	Prominent Results	Reference
1	2	3	4	5	6
Al 5083 L – 200 mm, W – 50 mm, T – 10 mm.	SiC (10 um), Al_2O_3 (3 um), Groove Method: GW – 3 mm, GD – 6 mm.	H – 13 Tool Steel, Flat shoulder, Square Probe: W – 6 mm, L – 6 mm, SD – 25 mm.	w – 400, 600, 800 rpm, v – 60 mm/min, TT – 3°, FSP passes – 2, Hybrid Ratio: (50%SiC, 50% Al_2O_3), (100%SiC) and (100% Al_2O_3).	The average Hardness values increased by 30% with increase in ceramic content. The maximum hardness value obtained at (SiC 50%, Al_2O_3 50%) hybrid ratio, 2 FSP passes and at 600 rpm. The higher wear resistance observed for composites with (SiC 50%, Al_2O_3 50%) hybrid ratio.	Zayed et al. (2019) [39]
Al 5083 T – 8 mm.	B_4C (>10 μm), MWCNT (avg. length – 1 μm, diameter 2 0-30 nm), Surface Blind Holes method: ϕ – 2 mm, depth – 3 mm, intercavity spacing – (8 mm, 10 mm).	H – 13 steel of collet diameter 16 mm, SD – 20 mm, conical threaded pin, PD – (4, 6 mm)), PL – 5 mm.	FSP pass: w – 750 rpm, v – 16 mm/min, TT – 2°, No. of pass – 1.	The Al 5083/B4C composite showed maximum rise of 20% increase in HV and 41% increase in UTS with 10mm inter – cavity distance. The hybrid Al 5083/MWCNT/B_4C composite showed intermediate increase in microhardness and tensile strength. The 10 mm inter – cavity distance proved better results than 8 mm.	Mahmood Khan et al. (2017) [40]
Al 5083 L – 140 mm W – 50 mm T – 5 mm.	Al_2O_3 (80 nm), TiO_2(15 nm), Groove Method: GW – 1 mm, GD – 2 mm.	52 HRC H13 tool steel, SD – 20 mm, threaded pin PD – 6 mm, PL – 3 mm.	FSP Pass: w – (500, 710, 1000 rpm), v – (20, 56 mm/min), TT – 3°, No. of passes – 2.	The higher UTS and hardness attained at 710 rpm and 20 mm/min as independent parameters. The hybrid composites had low friction coefficients and wear rates than that of base alloy.	Heiderpour et al. 2018 [41]

1	2	3	4	5	6
Al 5083 L – 250 mm, W – 100 mm, T – 5 mm.	CeO_2 (~50 nm), SiC (~80 nm), Groove Method: GW – 1.2 mm, GD – 2 mm, L – 230 mm.	H13 tool steel, concave shoulder, SD – 18 mm, threaded cylindrical pin, PD – 6 mm PL – 4.5 mm.	FSP two passes at: w – 800 rpm, v – 35 mm/min. FSP third pass at: w – 600 rpm, v – 45 mm/min. TT – 3°, for third pass changed AS to RS	The increasing no. of passes and changing direction of processing helped in distribution of reinforcements and improved SZ homogeneity. Improved wear performance for hybrid composite than base alloy and mono composites was reported due to The solid lubricating CeO_2.	M. Amra et al. 2018 [42]
Al 5083 – O T – 8 mm.	B_4C (30–60 nm), TiC (30–60 nm), Groove Method: GD – 3 mm, GW – 1 mm.	H – 13 steel tool, SD – 18 mm, cylindrical threaded pin, PD – 6 mm PL – 5 mm.	FSP Pass: w – 1000 rpm, v – 40 mm/min, No. of FSP Passes – 4 Hybrid Ratio: (100% B_4C), (100% TiC), (50% B_4C, 50% TiC).	Higher wear resistance for hybrid Al5083/B_4C/TiC composite than others; because of attained low coefficient of friction. The load bearing B_4C particles and solid lubricant TiC particles helped in improving the tribological and mechanical properties of the hybrid composites.	N. Yuvraj et al. 2016 [43]
Al 5052 – H32.	TiO_2(~30 nm), Groove Method: 210 mm long, GD – 4 mm, GW – (0.8, 1.2 mm).	H13 steel tool, Concave shoulder surface, SD – 18 mm, straight threaded cylindrical pin, PD – 5 mm, PL – 4 mm, thread angle – 30°.	capping pass: w – 1075 rpm, v – 30 mm/min FSP pass: w – 1200 rpm, v – 100 mm/min, No. of FSP passes – 6, F – 10 KN, TiO_2 – (~2, 3.5 vol%).	The UTS and YS improved by 90% and 31% than the base alloy. Fatigue strength improved by 33% and 28% for the Nano composites with TiO_2 vol % of 3.5 and 2 respectively. Ductility reduced up to 30%. Micro – cracks, micro – voids were observed on the fractured specimens after fatigue tests.	P. Sahandi et al. 2016 [44]
Al 5052 – H32 L – 210 mm W – 70 mm, T – 5 mm.	TiO_2 (~30 nm) Groove Method: GD – 3.5 mm, GW – 1.2 mm.	SD – 18 mm, threaded pin FSP tool PD – 5 mm, PL – 4 mm, pin threads depth – 0.5 mm, angle – 30°.	Capping pass: w – 1075 rpm, v – 30 mm/min, FSP pass: TT – 2.5°, w – 1200 rpm, v – 100 mm/min, No. of FSP passes – 4, TiO2 vol% – ~3.1%	Hybrid composite showed higher high temperature strength. Deformation activation energy at high temperatures had been increased significantly after FSP. Very fine hard particles produced through in – situ reaction during FSP had contributed reasonably to hard deformation behavior enhancement and thermal stability.	F. Khodabakhshi et al. 2014 [45]
Al 5083 L – 250 mm W – 100 mm T – 5 mm.	CeO_2 (30 nm), MWCNT (L – 10-20 µm, D – 10 – 20 nm), Groove Method: GW – 1.2 mm, GD – 2 mm.	52 HRC H13 tool steel, Cylindrical concave shoulder, SD – 18 mm, threaded cylindrical pin, PL – 4.5 mm, PD – 6 mm.	FSP passes: First two with w – 800 rpm, v – 35 mm/min. Third pass with w – 600 rpm, v – 45 mm/min, No. of FSP passes – 3, TT – 5°, and volume ratios used – 25, 50 and 75.	The higher mechanical properties were obtained for hybrid ratio of 75% CNT and 25% CeO_2. The average grain size in the processed zone decreased significantly after FSP. The CeO_2 nano particles helped in enhancing the resistance to the pitting corrosion; on the other hand cathodic natured CNT had deteriorated the resistance to pitting.	S.A. Hossieni et al. 2014 [46]
Al 5083 T – 5 mm, Groove Method W – 1.2 mm, D – 2 mm, L – 230 mm.	CeO_2 (50 nm), SiC (80 nm).	52HRC H13 tool steel, Concave shoulder, SD – 18 mm, threaded cylindrical pin, PL – 4.5 mm, PD – 6 mm.	FSP passes: first two (w – 800 rpm, v – 35 mm/min) Third pass (w – 600 rpm, v – 45 mm/min), TT – 3°, vol. ratios – 25:75, 50:50, 75:25.	The mono composite with 100% SiC had obtained highest tensile strength and hardness than other composites. The CeO_2 particles had helped in improving the pitting corrosion resistance by means of increasing the passivation range. The hybrid composite with volume ratio 25%SiC: 75%CeO_2 had shown the most optimum combination of mechanical properties and corrosion resistance.	M. Amra et al. 2015 [47]
Al 5083 – H116 T – 10 mm.	Al_2O_3 (80 nm), Gr (10–50 nm), Groove Method: GW – 1 mm, GD – 4.5 mm.	HRC51 H13 tool steel	FSP passes: w – 1250 rpm, v – 20 mm/min, TT – 3°, No. of pass – 3, Hybrid ratios – 25:75, 50:50. 75:25	Nano composites material with (75% Gr, 25% Al_2O_3) hybrid ratio had shown higher tensile properties but if application required both combination of good tensile and wear properties then (50% Gr, 50% Al_2O_3) hybrid ratio would be beneficial. Interparticle spacing of reinforcements inside composites had affected mechanical properties.	Mostafapour et al. 2013 [48]
Al 5083 T – 3 mm.	MoS_2 (5 µm), SiC (5 µm) Groove Method: GD – 2 mm, GW – 0.65 mm.	H13 steel, SD – 20 mm PD – 6 mm PL – 2.8 mm, TT – 3°.	FSP pass: w – 1250 rpm, v – 50 mm/min, No. of FSP pass – 1, powders weight ratio used – 2:1.	Microhardness shown by 100% SiC mono composite was higher. Hybrid composite exhibited higher wear resistance than other mono composites and base alloy. Friction coefficient was intermediate for hybrid composite compared to higher 100% SiC composite and others.	S. Soleymani et al. 2012 [49]

Al 5052 alloy was enhanced with the use of FSP at the cost of reducing ductility. Increasing TiO_2 concentration, greater yield and ultimate tensile strength were also achieved even though the ductility was slightly lost. It was noted that considerable grain refinement occurred on the aluminum alloy FSP, especially while titanium dioxide particles were used. The result of dynamic recrystallization leads to the growth of new and dislocation-free grains at earlier grain boundaries and deformation band interfaces. By Zener-Holloman pinning effect – MgO (50 nm), Al_3Ti (50 nm), TiO_2 (30 nm) particles hindered the rate of grain boundary movement throughout a fine-grained Al alloy matrix (<2 μm). The Al 5052 alloy's average grain size was around 49 μm, which was lowered to about 11 μm since 6-pass FSP.

In converse to Sahandi et al. [44], in another study Zayed et al. [39] found that the ductility of the material was significantly improved along with tensile strength for Al 5083-SiC/Al_2O_3 hybrid composite produced. The average micro hardness increased with content of ceramic particles. Reinforcement's distribution become more uniform and homogenous with increase in no. of stirring passes. Heiderpour et al. [41] produced Al5083-Al_2O_3/TiO_2 hybrid surface nano-composites. They noted that as per Hall-Petch equation, reducing the grain size contributed to rise in the hardness value. In conjunction to grain refinement, the improvement in micro-hardness value was due to direct reinforcement given to the matrix by these strong and hard reinforcements, which impeded the movement of the dislocations in the composite. The microhardness values obtained with this combination is one of the maximum results for Al 5xxx series as shown in Fig. 4.

Mostafapour et al. [48] found that nano composites produced with different hybrid ratios had shown different tensile properties for Al 5083-Gr/Al_2O_3 composites. Particle clustering in processed zone increased with rise in reinforcement volume percentage. Microhardness and UTS had shown two trends i.e. enhanced properties when mean inter-particle spacing is reduced up to specific hybrid ratio and deteriorated after further reduction in inter particle spacing of Alumina in the nano composites. They mentioned that if nano composites material had application with requirement of higher tensile properties then (75% Gr, 25% Al_2O_3) hybrid ratio would be best option. S. A. Hossieni et al. [46] fabricated Al 5083/CeO_2/CNT hybrid composites. They found higher mechanical properties for hybrid composite with (75% CNT, 25% CeO_2) combination than mono composites and base alloy. They mentioned that many strengthening mechanisms were present simultaneously. Average grain size in processed zone decreased significantly after FSP. Highest UTS of 396 MPa obtained for hybrid surface composite with (75% CNT, 25% CeO_2).

Halil Ibrahim Kurt [50] estimated effect of hybrid ratio and FSP machine parameters on tensile strength of Al 5083 using mathematical formulation model using Matlab. The experimental UTS results measured for Al 7075, Al 6061, Cu, Al 1016 and Al 5083 with various hybrid reinforcements reported by researchers in literature were used as training data for model. As per the findings, UTS increased with increasing CNT vol%, tool rotational speed and traverse speed. Reinforcement combinations used were CNT/ZrO_2/SiC/Gr/Al_2O_3 particles. Through mathematical model, (10% Gr, 5%ZrO_2) hybrid ratio showed maximum tensile strength for Al 5083 hybrid composites.

Ahemadifard et al. [51] fabricated the AA5083/Al_2O_3/TiO_2 hybrid nano composites and obtained improved mechanical properties. They found that the tensile behavior was changing according to the hybrid ratio of the reinforcements. The hybrid composite with (25% Al_2O_3 and 75% TiO_2) combination showed highest tensile strength and microhardness. The multipass FSP helped in distributing the reinforcements in the processes zone but still at some points agglomerated clusters were detected in the metallographic study. They attributed the reasons for improvements in mechanical properties to the stir mixing of hard ceramic nano particles in the intense plasticized zone during the fabrication process. The various strengthening mechanisms found to be present simultaneously.
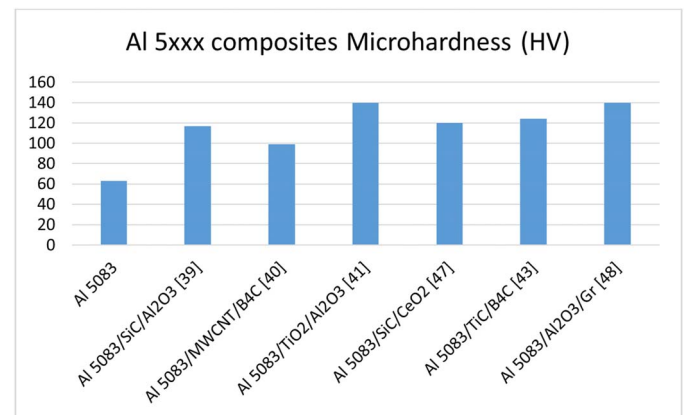

Fig. 3. Microhardness (HV) values of Al 5xxx hybrid surface composites
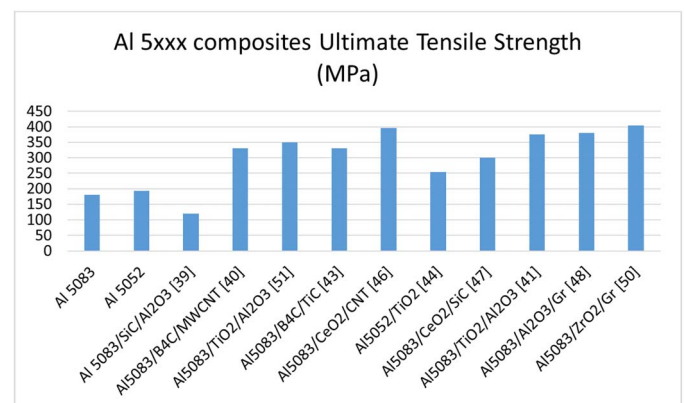

Fig. 4. Ultimate tensile strength of Al 5xxx hybrid surface composites

The attempts were made for improving the surface properties like wear rate and coefficient of friction of the Al 5xxx series alloys using approach of hybrid composites through FSP. The wear rates of Al 5xxx hybrid surface composites are enlisted in Table 4. Zayed et al. [39] improved wear resistance of Al 5083 by 40% for (SiC 50%, Al_2O_3 50%) combination. Reinforcement's distribution become more uniform and homogenous with

increase in no. of stirring passes. The consolidated SiC and Al_2O_3 ceramic particles resisted the plastic flow of the material by enhancing the material's strength and hardness at elevated temperatures. In addition, the SiC particles hold the material debris on the surface, and some of this debris got collected around the particles during wear by staying stable at those locations. Also these ceramic powders avoided severe contact between ball and the substrate surface and beard more load at their localized points.

TABLE 4

Wear rate of Al 5xxx based hybrid surface composites

Composite	Load	Wear rate	Reference
Al 5083-SiC/Al_2O_3	20 N	0.6 g/m	Zayed et al. [39]
Al 5083-Al_2O_3/TiO_2	20 N	0.28 mg/m	Heiderpour et al. [41]
Al 5083-Gr/Al_2O_3	24.8 N	48×10^{-6} g/m	Mostafapour et al. [48]

In another study, Soleymani et al. [49] dispersed SiC/MoS_2 powders uniformly within processed zone and without any imperfections in Al 5083 alloy. They found that the surface composite layer had been very well bonded with the substrate without any void defects. The lamellar structured MoS_2 got decreased in size after FSP compared to hard SiC powder. With soft solid lubricating effect, MoS_2 powder helped in enhancing wear resistance of hybrid composite. The main wear mechanisms observed in hybrid composites were light delamination as well as light abrasion mechanism.

Heiderpour et al. [41] for Al5083-Al_2O_3/TiO_2 hybrid composites found lower friction coefficients and wear rates than base alloy at 710 rpm and 20 mm/min parameters due to grain refinement and effective dispersion of reinforcements. As they mentioned, volume loss was inversely proportional to the hardness of the surface composite, as per the Archard's wear law. By enhancement in the surface nano-composite's micro-hardness, metal removal during sliding wear was declined. They observed further that as tool rotational speed increased, the wear rate of the composites also increased. Because the highest hardness of 140 HV were acquired for FSPed samples with 710 rpm and 20 mm / min, the minimum wear rate observed. Wear resistance increased with greater hardness values due to microstructure changes and grain refinement during FSP.

Hossieni et al. [46] found that CeO_2 nano particles helped in enhancing resistance to pitting corrosion by behaving as a cathodic inhibitors; on other hand CNT had deteriorated resistance to pitting due to cathodic nature. Similarly, Amra et al. [42,47] mentioned that CeO_2 helped not only to improve wear resistance but also to lower coefficient of friction due to its solid lubricating effect. In further investigations [47], they observed good interfacing between reinforcements and base alloy; with no defects in friction stirred zone. The CeO_2 particles had helped in improving the pitting corrosion resistance by means of increasing the passivation range. SiC has not shown the passivation effect due to its cathodic nature. As per results, the hybrid composite with (25% SiC and 75% CeO_2) has shown the most optimum combination of mechanical properties and corrosion resistance.

Thus for Al 5xxx based hybrid surface composites showed significant material properties enhancement with help of solid state friction stirring technique with embedding the reinforcements. The optimum FSP machine parameters used for successful fabrication of Al 5xxx based hybrid composites are enlisted in Table 5.

TABLE 5

Successful FSP machine parameters used for Al 5xxx hybrid surface composites

Composite	Tool rotational speed (w) rpm	Tool traverse speed (v) mm/min	No. of passes (P)	Authors
Al5083/B_4C/ MWCNT	750	16	1	Khan et al. [40]
Al 5083/ CeO_2/SiC	800	35	3	Amra et al. [42]
Al 5083/ B_4C/ TiC	1000	40	4	Yuvraj et al. [43]
Al 5052/ TiO_2	1200	100	6	Sahandi et al. [44]
Al 5052/ TiO_2	1200	100	4	Khodabakshi [45]

2.1.3. 6xxx series alloy

In 6xxx series Al alloys, main alloying elements are Mg and Si. They represents heat treatable and strain hardenable medium strength alloys with good weldability, high resistance to stress corrosion cracking and corrosion resistance. They are utilized in extruded forms and sheets in various automotive and aircraft applications. Ultimate tensile strength (UTS) ranges between 245 MPa-330 MPa for various grades of Al alloys available in this series [31]. The summary of Al 6xxx alloy based hybrid surface composites is given in Table 6 below.

From the literature reported, heat treatable Al 6xxx alloy's tribological behavior were found significantly improved by the researchers. The microhardness of this series alloys were improved as shown in Fig. 5. However the tensile strength of Al 6xxx series alloys were deteriorated after FSP as shown in Fig. 6. In one of the studies, Sharma et al. [52] emphasized that hybrid Al 6061/SiC/Gr composites had higher nano mechanical properties than mono composites. They observed interfacial bonding between base alloy and ceramic particles. They had main two observations, i.e. SiC particles had de-bonding phenomenon with Al matrix due to defects induced around these particles during FSP and residual stresses with edge disorder in graphite crystals were observed after FSP in the resultant composites. The Gr particles were sheared during FSP. They found that mean axial force during friction stirring increased for mono Al-Gr composite due to high thermal conductivity of graphite. They remarked that graphite layer and grain refinement helped in reducing interfacial and intergranular corrosion of hybrid composite. Despite of these effects, the nano-mechanical properties were found higher for the hybrid composites.

TABLE 6

A Summary of hybrid surface composites fabrication on Al 6xxx alloys

Base Material and size	Reinforcement and Preplacement Method	Tool Material and Specifications	FSP Process Parameters	Prominent Results	Reference
1	2	3	4	5	6
Al 6061 T – 6 mm.	SiC (~100 μm), Graphite (~44 μm), Groove Method: GW – 3 mm, GD – 2 mm.	H13 tool with flat shoulder, SD – 25 mm, square pin: W – 5 mm, L – 5 mm, H – 5 mm.	FSP pass: w – 1800 rpm, 2200 pm, and 2500 rpm used for plunge depth of – 0.2 mm, 0.3 mm and 0.4 mm at constant v – 25 mm/min, Hybrid Ratio: (50% SiC, 50% Gr), (SiC 100%) and (Gr 100%).	Hybrid reinforcements helped in improving mechanical properties. Optimum improved mechanical properties are obtained at 2200 rpm and 25 mm/min. Exfoliation of Graphite into graphene and presence of residual stresses was confirmed using Raman Spectroscopy.	Abhishek Sharma et al. (2018) [52]
Al 6061 L – 150 mm, W – 100 mm T – 6 mm.	Al_2O_3 (<500 nm), TiB_2 (<500 nm) Groove Method: GW – 2mm, GD – 3.5 mm.	H13 steel tool, SD – 16 mm, Pin profiles: straight cylindrical, threaded cylindrical, tapered cylindrical, square, triangular pin, PL – 4 mm, PD – 5 mm.	FSP pass: w – 1500 r/min, v – 25 mm/min, No. of pass – 1.	They found that for FSP using square and triangular pin profile hardness and wear properties highly improved because of more uniform distribution, fine grain size, better flow of stirred material than other pin profiles.	V.M. Khojasteh-nezhad et al. (2017) [53]
Al 6082 L – 100 mm W – 50 mm T – 10 mm.	TiB_2 (~20 μm), BN (~200 nm) Groove Method: GW – 1.2 mm GD – 5 mm.	62HRC HCHCr steel, SD – 18 mm, cylindrical threaded pin, PD – 6 mm, PL – 5.5 mm.	FSP pass: w – 1600 rpm, v – 60 mm/min, F – 10 KN, No. of passes – 2 with changing AS to RS, Hybrid ratios: 100% TiB2, (50% TiB_2, 50% BN) and 100% BN.	Improved wear resistance obtained in fine average grain sized (6μm) hybrid composites. Micron sized TiB2 particles were fractured during FSP to change their morphology. The counter face wear reduced because of less Fe percentage in wear debris. The Fe percentage in wear debris of hybrid composite (5.4%) was less than the mono AMC with TiB_2 (9.2%).	R. Palanivel et al. (2016) [54]
Al 6063 L – 200 mm W – 70 mm T – 10 mm.	B_4C (7 μm), Ti (40-60 μm), B (2 μm), Al (63 μm) Groove Method: GD – 4.5 mm, GW – 1 mm.	cylindrical threaded tool, SD – 18 mm, PD – 6 mm, PL – 4.5 mm.	FSP pass: Three passes with w – 1000 rpm and fourth with w – 710 rpm, v – 40 mm/min TT – 2°.	The addition of B_4C and TiB_2 powders improved the hardness and the wear resistance. The AMC with 100% TiB2 reinforcement held maximum hardness and wear resistance because of protective oxide (Fe_2O_3) metal matrix layer over the surface. The wear debris with smaller sized flakes observed for hybrid composites.	Mohammad Narimani et al. 2016 [55]
Al 6061 T – 6 mm.	Al_2O_3 (500 nm), TiB_2 (500 nm) Groove Method: GW – 2 mm GD – 3 mm.	H – 13 steel tool, SD – 16 mm PD – 5 mm PL – 3.5 mm.	FSP pass: w – 1250 rpm, v – 16 mm/min, No. of passes – 1 to 4, Powders Wt. 1 g/cm length of the groove.	Microhardness values increased with number of FSP passes. Wear resistance after four FSP passes improved significantly to produce hybrid composites. Presence of TiB_2 hard particles, avoiding defects and solid lubricant Al_2O_3 within surface layers has contributed cumulatively to improve wear resistance of hybrid nano composites.	Reza Vatankhah Barenji et al. 2015 [56]
Al 6061 L – 100 mm W – 50 mm T – 6 mm.	Al_2O_3, Gr (avg. size. 95 nm) Groove Method GW – 1 mm GD – 1.5 mm.	HCHCr steel tool, SD – 18.5 mm, shank diameter – 15 mm, threaded cylindrical pin, PD – 4.5, PL – 3 mm.	Hybrid Ratio – Al_2O_3 – 0.5 wt%, Gr (0, 2, 4, 6, 8 and 10 wt%)	Composites with combination (6% Al_2O_3, 0.5% Gr) had shown higher mechanical properties in terms of hardness and wear resistance. Dynamic recrystallization due to intense super plastic deformation during stirring had significantly refined grains sizes and helped in uniform dispersion of ceramic particles.	T. Prakash et al. 2014 [57]

1	2	3	4	5	6
Al 6061 – T6 T – 4 mm.	SiC, Gr (20 μm) Groove Method GW – 3 mm, GD – 3 mm.	H13 tool steel, screwed taper pin profile, with SD – 24 mm, PD – 8 mm PL – 3.5 mm.	v – 40 mm/min, F – 5 KN, TT – 2.5°, Hybrid Ratio – (6 vol%), Gr (3 vol%).	During wire EDM cutting FSPed hybrid composites tool wear rate decreased with rise in pulse off time; surface roughness decreased with rise in current i.e. increased spark discharge energy. Material removal rate of produced composites enhanced with increased pulse off time and current.	Murahari Kolli et al. 2013 [58]
Al 6061 – T6, T – 4 mm.	SiC, Gr, Al_2O_3, (avg. size – 20 μm) Groove Method GW – 3 mm, GD – 3 mm 2 mm far away from the center line.	H13 tool steel SD – 24 mm, screwed taper pin, PD – 8 mm PL – 3.5 mm.	w – 900 r/min, v – 40 mm/min, F – 5 KN, TT – 2.5° Hybrid Ratio: (SiC: Gr) (SiC: Al_2O_3) vol. ratio (8%:4%).	The Al 6061/SiC/ Al_2O_3 composite had shown higher hardness than AL6061/SiC/ Gr combination due to hard nature of the Al_2O_3 than Gr powder. Wear resistance of SiC/Gr combination was higher than SiC/ Al_2O_3 case because of higher solid lubricating nature of the Gr than Al_2O_3 powder. The SiC/Gr combined hybrid composites showed thin layer of mechanically mixed reinforcements within hybrid composite which acted as solid lubrication to reduce wear rate.	A. Devaraju et al. 2013 [59]
Al 6061 – T6 T – 13 mm.	Cr_2O_3 Atmosphere plasma spray.	H13 steel v – 100 mm/min ω – 630 rpm TT – 3°.	w – 630 rpm, v – 100 mm/min, TT – 3°, No. of passes – 6.	The $Al_{13}Cr_2$ and $Al_{11}Cr_2$ intermetallics dispersion within the processed zone had helped in enhancing wear resistance of hybrid nano composites produced. FSPed base alloy without reinforcement also shown higher wear resistance due to reduction in number of hardening precipitates due to severe super plastic deformation.	S.R. Anvari et al. 2013 [60]
Al 6360 T – 10 mm, L – 100 mm.	TiC (~2 m), B_4C (~3 m) Groove Method: GW – 0.5 mm GD – 5.5 mm.	62 HRC – HCHCr steel tool, cylindrical threaded pin, SD – 18 mm, PD – 6 mm, PL – 5.8 mm.	w – 1600 rpm, v – 60 mm/min, F – 8 KN, No. of passes – 2 with changing AS to RS Hybrid Ratio – 100% TiC, (75% TiC+25% B_4C), (50% TiC + 50% B_4C), (25% TiC+75% B_4C) 100% B_4C.	The all hybrid composites showed less wear rate than the base alloy. The (50%TiC, 50% B_4C) combined hybrid composite had lowest wear rate amongst them. Equi – axed flakes received as wear debris of the hybrid surface composite. The iron content within wear debris of (50%TiC, 50% B_4C) hybrid composites were low; thus reduced counterface wear.	C. Maxwell Rejil et al. 2012 [61]
Al6061 L – 100 mm W – 50 mm T – 20 mm.	TiN (50 nm), Gr (10-20 μm) Groove Method: U shape groove, GD – 2 mm, GW – 1 mm.	45HRC Steel SD – 20 mm , cylindrical pin, PD – 4 mm, PL – 3 mm.	w – 1800 rpm, v – 80 mm/min, TT – 3°.	Higher wear resistance for hybrid TiN/ Gr volume ratio of 0.2. Interestingly, they observed that the hardness was not uniform throughout the depth of the processed zone along the thickness. The higher microhardness reported at surface layer 2 mm below from the processed surface.	M. Mansumi et al. 2012 [62]

Murahari Kolli et al. [58] studied wire EDM cutting process of Al 6061-T_6/SiC/Gr composites. They found that for cutting of hybrid composites; tool wear rate decreased with rise in pulse off time and surface roughness decreased with rise in current i.e. increased spark discharge energy. Material removal rate of produced composites enhanced with increased pulse off time and current.

Khojastehnezhad et al. [53] used different FSP tool pin profiles such as- simple and threaded straight cylindrical, square, taper and triangular for developing Al 6061/ Al_2O_3/TiB_2 composites using FSP. They found that for FSP using square and triangular pin profile, hardness and wear properties highly improved because of more uniform particles distribution, fine and equiaxed grain structure and better flow of the stirred material than other pin profiles. In another study, Berenji et al. [56] used
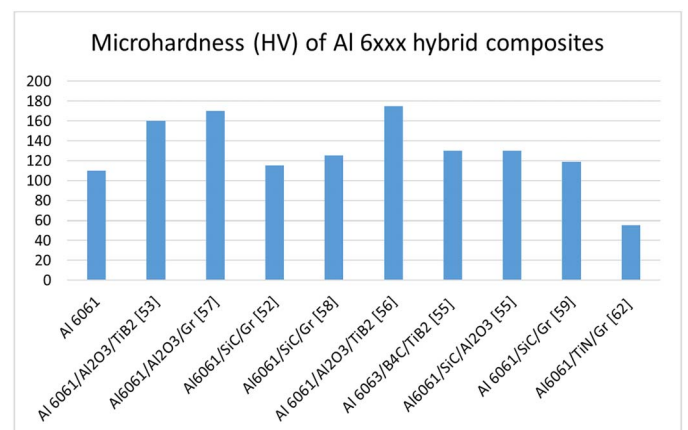

Fig. 5 Microhardness (HV) of Al 6xxx alloys based hybrid surface composites

multipass FSP strategy for synthesizing Al 6061/Al$_2$O$_3$/TiB$_2$ hybrid composites. They pointed out that multi-pass FSP helped in distribution of nano particles and reduction of average grain size in processed zone. They found that hardness values increased with increase in number of FSP passes used for fabrication of composites.

R. Palanivel et al. [54] observed uniform distribution of reinforcements and pointed out that distribution of particles was independent of location in stir zone of Al 6082/TiB$_2$/BN composites. Fine average grain size of 6 μm obtained in hybrid composites. Micron sized TiB$_2$ particles were fractured during FSP to change their morphology and shape due to intense plasticization. BN particles remained same as that of as received size. Narimani et al. [55] used ball milled B$_4$C particles and TiB$_2$ particles for fabricating Al 6063/B$_4$C/TiB$_2$ composites. With addition of B$_4$C and TiB$_2$ powders further improved hardness Composite with 100% TiB$_2$ reinforcement held maximum hardness because of protective oxide layer over surface of resultant composites.

Kumar et al. [63] investigated FSP tool rotational speed effects on mechanical properties of Al 6061/SiC-Gr/SiC-Al$_2$O$_3$ hybrid composites. They obtained higher microhardness for SiC/ Al$_2$O$_3$ combination due to Zener pinning effect after dispersion of these reinforcements. Similarly in another study, Devaraju et al. [59] found that out of Al 6061/Sic-Gr/SiC- Al$_2$O$_3$ hybrid composites, SiC/ Al$_2$O$_3$ combination shown higher hardness than SiC/Gr combination due to hard nature of Al$_2$O$_3$ than Gr powder. In another study of fabrication of Al 6061/ Al$_2$O$_3$/Gr composites by Prakash et al. [57], they used weight percentage of Al$_2$O$_3$ (0, 2, 4, 6, 8 and 10) with constant Gr 0.5% weight percentage. They found that (6% Al$_2$O$_3$, 0.5% Gr) had shown higher hardness than others. They concluded that dynamic recrystallization due to intense super plastic deformation during stirring had significantly refined grains sizes and helped in uniform dispersion of ceramic particles.

Mansumi et al. [62] produced Al 6061/TiN/Gr composites through friction stirring. They pointed out that combination of graphite with TiN powder had enhanced distribution of hard TiN powder; thus reduced agglomeration of ceramic particles. Hard TiN improved load bearing capacity in the composites. They
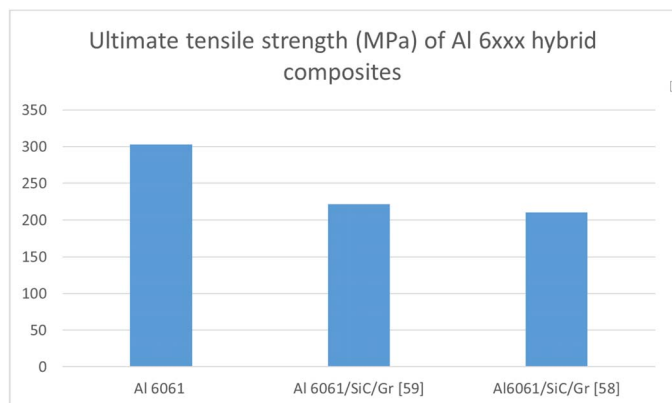
observed that hardness was not uniform throughout depth of processed zone along thickness. Higher microhardness reported at surface layer 2 mm below from processed surface.

The Al 6xxx series alloys were processed with optimum FSP machine parameters as given in Table 7. The combination of hard and soft ceramic powders were used so as to balance both mechanical as well as tribological behavior. The multi pass strategy was used for further enhancement in FSPed composites.

TABLE 7

Successful FSP machine parameters used for Al 6xxx hybrid composites

Composite	Tool rotational speed w (rpm)	Tool Traverse speed v (mm/min)	No. of passes (P)	Reference
Al 6061/SiC/Gr	2200	25	1	Sharma et al. [52]
Al 6061/Al$_2$O$_3$/TiB$_2$	1500	25	1	Khojastehne-zhad et al. [53]
Al 6061/Al$_2$O$_3$/TiB$_2$	1250	16	1	Berenji et al. [56]
Al 6082/ B$_4$C/TiB$_2$	1600	60	2	Palanivel et al. [54]
Al 6063/ B$_4$C/TiB$_2$	1000	40	4	Narimani et al. [55]
Al 6061/ SiC/Gr	900	40	1	Kumar et al. [63]
Al 6061/Al$_2$O$_3$/Gr	700	60	1	Prakash et al [57]
Al6061/Cr$_2$O$_3$	630	100	1	Anvari et al. [60]

The wear rate of Al 6xxx based hybrid composites were decreased satisfactorily by using different reinforcements as shown in Table 8. However, loading condition while performing the tribological testings is matter of concern since at some critical value the wear mechanism turns from soft wear to severe wear mechanism.

TABLE 8

Wear rate of Al 6xxx hybrid surface composites

Composite	Load	Wear Rate	Reference
Al 6061/Al$_2$O$_3$/TiB$_2$	50N	0.4 mg/m	Khojastehnezhad et al. [53]
Al 6061/Al$_2$O$_3$/TiB$_2$	50N	0.4 mg/m	Berenji et al. [56]
Al 6082/ B$_4$C/TiB$_2$	20 N	13×10^{-5} mm^3/Nm	Palanivel et al. [54]
Al 6063/ B$_4$C/TiB$_2$	15 N	0.01 mg/m	Narimani et al. [55]
Al 6061/ SiC/Al$_2$O$_3$	40 N	2 mm^3/m	Kumar et al. [63]
Al6061/Cr$_2$O$_3$	10 N	0.02 mg/m	Anvari et al. [60]
Al 6360/TiC/B$_4$C	20 N	300×10^{-5} mm^3/m	Rejil et al. [61]

Fig. 6 Ultimate tensile strengths of Al 6xxx based hybrid surface composites

Berenji et al. [56] fabricated Al 6061/ Al$_2$O$_3$/TiB$_2$ hybrid composites and obtained improved wear resistance than base

alloy. They obtained significantly improved wear resistance after four FSP passes to produce hybrid composites. Adhesive and abrasive mechanism was observed in wear against a steel disk in wear tests. The presence of ceramic TiB_2 hard particles, lack of cavity like defects and solid lubricating nature of Al_2O_3 within surface layers has contributed cumulatively to improve wear resistance of hybrid nano composites. Narimani et al. [55] found that with addition of B_4C and TiB_2 powders the wear resistance of further improved for Al 6063 composites. Composite with 100% TiB_2 reinforcement held wear resistance because of protective oxide layer over surface. Wear debris with smaller sized flakes observed for hybrid composites than Al 6063 plates; so less affinity to agglomeration.

Kumar et al. [63] found that and soft solid lubricants Gr and Al_2O_3 particles helped in improving wear properties of produced hybrid Al 6061/SiC-Gr/SiC-Al_2O_3 composites. Hybrid composites with SiC/Gr combination shown reduced wear rate because of hard load bearing SiC particles and solid lubricant Gr particles. In case of SiC/Al_2O_3, wear debris obtained were more with abrasion wear mechanism because of pulling out the hard particles on steel disk during wear tests. Devaraju et al. [59] confirmed same results for Al 6061/Sic-Gr/SiC-Al_2O_3 composites. So that wear resistance of SiC/Gr combination was higher than SiC/Al_2O_3 case because of higher solid lubricating nature of Gr than Al_2O_3 powder. The SiC and Al_2O_3 particles showed good interfacing with base alloy in hybrid surface composite. SiC/Gr combined hybrid composites showed thin layer of mechanically mixed reinforcements within hybrid composite which acted as solid lubrication to reduce wear rate.

Anvari et al. [60] used Al 6061/Cr-O materials, Cr_2O_3 is initially converted to pure Cr and Al_2O_3 during friction stirring. These phases reacted with Al substrate further produced $Al_{13}Cr_2$ and $Al_{11}Cr_2$ intermetallics. These hard intermetallics dispersion within processed zone had helped in enhancing wear resistance of hybrid nano composites produced. They found that after FSP of base alloy without putting reinforcement, wear resistance was higher owing to reduction in number of hardening precipitates during friction stirring.

Rejil et al. [61] found that all Al 6063/TiC/B_4C hybrid composites showed less wear rate than base alloy. However, the (50%TiC, 50% B_4C) combined hybrid composite had lowest wear rate amongst them. They observed that equi-axed flakes received as wear debris of hybrid surface composite. Iron content within wear debris of (50%TiC, 50% B_4C) hybrid composites were low; thus reduced counterface wear. Mansumi et al. [82] fabricated Al 6061/TiN/Gr composites through FSP. They observed that wear resistance was varying with variation in hybrid ratio of TiN and Gr particles. Hard TiN improved load bearing capacity where as soft Gr added solid lubricating effect to mechanically mixed layers after severe plasticization action in FSP. They obtained higher wear resistance for hybrid TiN/ Gr volume ratio of 0.2.

2.1.4. 7xxx series

Al 7xxx series alloys are age hardenable and strain hardenable with Zn-Mg-Cu as alloying elements. They are amongst super high strength alloys used in many structural applications in aerospace, ship building, automotive and defense equipment industry. Their UTS ranges 220 MPa to 600 MPa in various grades of this series. These are favorable material because of very high specific strength and high toughness [31]. Summary of Al 7xxx alloys based hybrid composites fabrication using FSP is mentioned in Table 9 below.

The phenomenon of dissolution of large precipitates already present in base alloys during FSP was confirmed by Naeem [65] and Soleymani Mahmoud et al. [67], which deteriorated microhardness of resultant composites. Thus subsequent heat treatments were performed on the composites to regain precipitates in the base alloys. Naeem [65] fabricated Al 7075 surface composites through FSP pulverization of ball milled Ni and (Al, Zn, Cu, Mg) particulates into the substrate. Processed samples were applied with T_6 aging and homogenization treatments. Microstructural characterization confirmed that average grain size decreased up to 70% after FSP with equiaxed grains. The ball milled highly energized Ni powder and increased no. of Al-Ni intermetallics changed microstructure and led to increased dislocation density. Thus composites shown higher hardness values than as received Al 7075 alloy. Soleymani Mahmoud et al. [67] synthesized Al 7075-T_6/SiC/BN hybrid composites with multipass FSP (6) to improve wear resistance and hardness of base alloy. They observed that hybrid composites had lower microhardness and wear resistance than as received Al7075-T_6 alloy; since precipitates got dissolved with intense superplastic deformation in FSP. Finally after application of T6 heat treatment again on the Al 7075/SiC/BN hybrid composites; they showed higher hardness values almost by one third than base Al 7075-T_6 alloy. Microstructural characterization confirms that micron sized SiC and nano sized BN had been distributed uniformly after repetitive 6 FSP passes.

Azadi Mina et al. [68] noted that soft solid lubricant nature of MoS_2 was most contributive factor from improvement of wear resistance in the developed Al7075/TiC/MoS_2 hybrid composites. However hardness of hybrid Al 7075/TiC/MoS_2 composite was less than that of Al7075/TiC composite due to presence of soft solid lubricant MoS_2 powder. However they didn't mentioned any precipitates dissolution phenomenon responsible for drop in the microhardness of the composites.

The addition of (B_4C, MoS_2) [66] and (B_4C, TiB_2) [64] reinforcements using FSP helped in improving the ballistic properties of Al 7075 and Al 7005 respectively. Sudhakar et al. [66] found that hard and load bearing nature of B_4C, solid lubricant nature of MoS_2 have helped in achieving desirable wear and ballistic properties. They mentioned that poor tribological properties of Al alloys can be preferably improved more with FSP than other fusion based surface engineering methods. Nitinkumar Pol et al. [64] found that tough core of matrix and hard ceramic particles have improved ballistic resistance. The lowest depth of penetra-

A Summary of hybrid surface composites fabrication on Al 7xxx alloys

Base Material and size	Reinforcement and Preplacement Method	Tool Material and Specifications	FSP Process Parameters	Prominent Results	Reference
Al 7005 L – 150 mm W – 100 mm T – 8 mm.	TiB$_2$ (3 μm), B$_4$C (3 μm), Surface Blind Holes Method: ϕ – 1.5 mm, depth – 3 mm.	H13 tool SD – 18 mm, with straight cylindrical pin: PD – 6 mm, L – 4 mm.	w – 750 rpm, v – 50 mm/min, FSP passes – 2 with changing AS – RS, Hybrid Ratio: (50%TiB$_2$, 50%B$_4$C), (75%TiB$_2$, 25%B$_4$C) and (25%TiB$_2$, 75%B$_4$C)	All hybrid composites showed nearly same microhardness (170 HV) but higher than the base alloy (90 HV). Improved ballistic resistance observed in hybrid composites than base alloy due to presence of hard ceramic particles. Hybrid composite with (25%TiB$_2$, 75%B$_4$C) combination showed least steel projectile penetration (20 mm) compared to others.	Nitinkumar Pol et al. (2018) [64]
Al 7075 T – 13 mm L – 90 mm W – 20 mm.	Al, Zn, Mg, Cu, Ni particles Groove Method: V shape.	Stainless – steel tool, threaded tapered pin, flat shoulder.	v – 39 mm./min, w – 2300 rpm, Ageing Treatment (T6)	The FSPed composites shown higher hardness values than as received Al 7075 alloy. Avg. grain size decreased up to 70% after FSP with equiaxed grains. Ball milled highly energized Ni powder and increased no. of Al – Ni intermetallics changed circumstances and led to increased dislocation density.	Haider Tawfiq Naeem et al. (2017) [65]
Al 7075 – T6 L – 500 mm W – 500 mm T – 40 mm.	B$_4$C (30, 60, 160 μm), MoS$_2$ Surface Blind Holes Method.	H – 13 steel tool, straight cylindrical, SD – 20 mm, PL – 3 mm, PD – 6 mm.	w – 960 rpm, v – 50 mm/min, plunge speed – 30 mm/min.	Ballistic performance and wear resistance increased significantly in case of hybrid composites than other mono composites and base alloy. The hybrid composites showed very low coefficient of friction. The B$_4$C of size 30 μm along with MoS$_2$ gave optimum results due to load bearing and solid lubricant nature respectively.	I. Sudhakar et al. (2014) [66]

tion and improved mass efficiency factor (1.6 times) obtained for Al7005-(B$_4$C 75%, TiB$_2$ 25%) hybrid composite than base metal and other composites.

As per literature reported above on Al 7xxx series hybrid surface composites, it is noted that microhardness, wear resistance and ballistic properties were improved in respective base alloys. However emphasized studies on tensile behavior of these composites are not yet reported.

2.2. Hybrid reinforced cast aluminium composites

The cast aluminium alloys are utilized in many areas including automotive industry due to their comparatively low melting temperature, good fluidity, better surface finish and low solubility of gases (except H$_2$). They are heat treatable as like wrought Al alloys [31]. Researchers used A356 [69,70], LM25 [71] and A413 [72] cast alloys as base material and reinforced with various ceramic particles to investigate improvements in mechanical properties. Table 10 summarizes fabrication of as cast hybrid composites with FSP.

During processing of A356, Akbari et al. [69] and Alidokht et al. [70] found that intense plasticization due to friction stirring resulted in defragmentation of Si particles and alloy dendrites. Thus, average grain size had decreased significantly; grains became more fine and equiaxed. Akbari et al. [69] fabricated A356/SiO$_2$/Al$_2$O$_3$ and found almost doubled microhardness with (20% SiO$_2$ and 80% Al$_2$O$_3$) combined hybrid composite than base A356 alloy. Increase in SiO$_2$ nano powder percentage from 0 to 100% had decreased microhardness consistently. Wear

resistance had increased by 35% than base A356 alloy with (20% SiO$_2$ and 80% Al$_2$O$_3$) combined hybrid composite. Alidokht et al. [70] fabricated A356/SiC/MoS$_2$ and found that presence of soft MoS$_2$ particles decreased hardness of hybrid composites. They also reported higher wear resistance and lower coefficient of friction for hybrid composite than mono SiC composite with base alloy. It was due to stable solid lubricating thin film generated in mechanically mixed layer with presence of MoS$_2$ particles.

Gurusamy et al. [71] fabricated LM25/SiC – Al$_2$O$_3$ and LM25/B$_4$C – Al$_2$O$_3$ composites and found that hybrid composites with B4C – Al$_2$O$_3$ combination had higher mechanical properties than SiC – Al$_2$O$_3$ combination. With decreasing tool rotational speed and traverse speed, reinforcement dispersion have decreased. They mentioned that increasing width of groove for deposition of reinforcements have no significant effect on powder distribution in stir zone. M. Janbozorgi et al. [72] synthesized A413/SiC/MoS$_2$ hybrid composite and found improved tribological behavior due to lubricating effect of MoS$_2$ particles. Wear rate and coefficient of friction decreased due to less adhesive mechanism amongst metallic particles in mechanically mixed layers incorporating MoS$_2$ particles in composite. Hardness of hybrid composite was less than Al/SiC composite due to incorporating soft solid lubricant MoS$_2$ particles.

3. Summary

The approach of fabricating hybrid surface composites on Al alloy substrates via FSP has gained much ground for improving their mechanical, tribological and corrosion resistive

TABLE 10

A Summary of hybrid surface composites fabrication on cast aluminium alloys

Base Material and size	Reinforcement and Preplacement Method	Tool Material and Specifications	FSP Process Parameters	Prominent Results	Reference
A413 Al – Si Alloy T – 8 mm W – 60 mm L – 80 mm.	SiC (7 μm), MoS$_2$ (10 μm), Groove Method: GD – 3 mm, GW – 2 mm.	H – 13 tool steel, columnar shape, SD – 16 mm, PD – 6 mm, PL – 3 mm.	v – 25 mm/min. w – 1600 rpm, TT – 3°, No. of Passes – 1.	The wear rate and coefficient of friction decreased due to less adhesive mechanism amongst metallic particles in mechanically mixed layers incorporating MoS$_2$ particles in the composite. The hardness of the hybrid composite was less than the Al/SiC composite due to incorporating soft solid lubricant MoS2 particles.	M. Janbozorgi et al. (2017) [72]
A356 T – 10 mm.	ZrO$_2$, SiC, B$_4$C, TiC Groove Method.	threaded pin, thread pitch – 1 mm, PD – 6 mm, SD – 18 mm, v – 8, 32, 80 mm/min w – 800, 1200, 1600 rpm.	FSP tool tilt angle, the penetration depth, and automatic plunging speed were kept constant at TT – 3, PL – 3.5 mm, v – 6 mm/min, No of passes – 4 with changing AS to RS.	The needles shape Si particles were broken into very fine particles due to intense plasticization. Almost doubled microhardness reported with (20% SiO2 and 80% Al$_2$O$_3$) combined hybrid composite than the base A356 alloy. The SiO2 nano powder percentage rise from 0 to 100% had decreased the microhardness consistently. The wear resistance had increased by 35% than base A356 alloy with (20% SiO$_2$ and 80% Al$_2$O$_3$) combined hybrid composite.	Mostafa Akbari et al. (2017) [69]
LM25 L – 160 mm, W – 50 mm, T – 34 mm.	SiC – Al$_2$O$_3$, B$_4$C – Al$_2$O$_3$, Groove method: groove GW – 1.4 mm, GD – 2 mm, at 1 mm offset to center line of the toolrotation on AS.	Straight cylindrical threaded pin tool.	v – 40 mm/min, F – 5 KN, TT – 2.5.	They found that the hybrid composites with B$_4$C – Al$_2$O$_3$ combination had higher mechanical properties than SiC – Al$_2$O$_3$ combination. They found uniform distribution of the reinforcements in the LM25 with the help of SEM testing. With decreasing tool rotational speed and traverse speed, reinforcement dispersion have decreased.	P. Gurusamy et al. (2015) [71]
A356, T – 10 mm.	SiC (30 μm), MoS$_2$ (5 μm) Groove Method.	H – 13 tool steel, columnar Shape, SD – 20 mm, threaded Pin, PD – 6 mm, PL – 3.7 mm pitch distance – 1 mm.	w – 1600 rpm, v – 50 mm/min, No. of passes: 1.	After FSP more fine and equiaxed grain structure obtained. The higher hardness for mono composite with SiC than the hybrid composite and base alloy; due to the inclusion of hard SiC particles. The presence of soft MoS$_2$ particles decreased the hardness in the hybrid composite. They reported higher wear resistance for the hybrid composite than the mono SiC composite with base alloy due to the stable solid lubricating thin film generated in the mechanically mixed layer.	S. A. Alidokht et al. (2011) [70]

properties successfully. The functionality of FSP to encapsulate desirable reinforcement particles into Al alloys processed below melting point temperature is now well established. After looking at the literature reported on fabrication of hybrid surface MMCs using FSP involving both in-situ and ex-situ approach, it's noted that fabrication by both routes are complex because it involves many process parameters. The Al alloys showed changed responses for comparable process parameters merely due to their different nature of metallurgical and structural behavior and thus it becomes essential to know the response of each alloy type to the respective processing conditions thoroughly. Thus this systematic review on Al hybrid composites fabrication and subsequent material properties variations via FSP technique is presented and various aspects are summarized.

The effect of FSP process parameters on tensile properties varied for heat treatable and non-heat treatable Al alloys. For 1xxx and 5xxx series based hybrid surface composites, the tensile strengths have been increased compared to base alloys.

The use of combination with load bearing hard ceramic particles and solid lubricant soft particles has shown improvements in both mechanical and tribological properties. The ball milling energization of reinforcements has shown significant effect on increasing the in situ reaction and improving the tensile strength of resultant composites. For heat treatable 6xxx and 7xxx series based hybrid surface composites, the tensile strength improvement is not reported, rather decrease in tensile strength due to dissolution of the large precipitates has been observed. Thus it emphasizes need of the heat treatment after FSP to regain the vanished precipitates into the base alloy. However for the heat treatable Al alloys, improved microhardness, ballistic properties, high temperature strength and tribological behavior obtained with various reinforcement combinations.

Many deposition methods for preplacing reinforcements on surface of base alloy were reported like groove method, surface blind holes method, mechanical alloying and plasma spraying method. Different groove shapes e.g. square groove, rectangular

groove, v shape groove etc. have been used. Blind holes with different diameters and depth were used by researchers for deposition of reinforcements. The various blind holes patterns on surface of base alloy with varying intercavity spacing was also reported in literature. Out of these preplacement methods, groove method is more popular because of easy implementation compared to other methods. However, surface blind holes method has less probability of powder wastage due to blowing during processing as the shoulder covers the upcoming hole before processing. The selection of intercavity spacing is crucial in order to maintain continuity of composites.

Generally, it is noted that selection of reinforcements for hybrid composites was combination of hard ceramic and soft solid lubricating particles to get balanced material properties. The FSP functionality with hybrid reinforcing strategy have shown presence of several strengthening mechanisms simultaneously in the material. The grain size strengthening by Orowan mechanism, work hardening due to strain misfit between reinforcements and base metal, increase in dislocation density due to coefficient of thermal expansion (CTE) mismatch and resistance to dislocation motions due to angled grain boundaries have been reported. The disintegration of precipitates in heat treatable Al alloys due to FSP has decreased the resultant material strength.

Various types of reinforcement materials have been used by researchers and found their effect on resultant hybrid surface composites. In this review, use of SiC, TiB_2, B_4C, Al_2O_3, Gr, MoS_2, Fe_2O_3, TiC, BN, CeO_2, TiO_2, TiN, GO (graphene oxide) and Cr_2O_3 powders have been reported. These particles have shown their own effect on resultant hybrid surface composites. Inclusion of hard SiC, B_4C, TiC, TiN particles helped in improving the hardness and strength of composites due to their load bearing nature and ability to activate different strengthening mechanisms. The TiB_2 ceramic particles have helped in improving wear properties, hardness and ballistic properties of composites. The solid lubricating nature of Gr, Al_2O_3, MoS_2, BN, TiC and CeO_2 has helped in improving tribological properties of resultant composites. The conversion of Gr into multilayered Graphene using FSP is reported and has helped in improving hardness and tensile properties of base alloy. The GO (graphene oxide) coated SiC has significantly contributed to increase in strength of material. CeO_2 nano particles helped in enhancing resistance to pitting corrosion by behaving as a cathodic inhibitors in hybrid composites. TiO_2 has been utilized as precursor material for synthesis of Al_3Ti and MgO reaction products in base alloys. Cr_2O_3 has been utilized as initial material for in-situ reaction with base alloy to develop $Al_{13}Cr_2$ and $Al_{11}Cr_2$ intermetallics in composites. MW-CNT has helped in increasing microhardness, UTS, wear resistance but deteriorated pitting corrosion resistance due to its cathodic nature in produced hybrid composites using FSP.

The triangular and square profile tools facilitated high dispersion in stir zone, however particle breaking was also reported. The tapered cylindrical threaded pin profile facilitates material flow not only in horizontal direction but also vertically along pin length. Multi pass FSP ensures more homogenous distribution of particles. The particles breaking increases with increase in number of passes. The multipass strategy improved the material strength in case of non-heat treatable Al alloys where-as decreased in case of heat treatable Al alloys.

Many challenges are remaining in this field that can be tackled in future research attempts. There is need to define general correlation model between various designed tool parameters and deposition method parameters also among FSP machine parameters and deposition method parameters in order to get defect free homogenous composites. FSP technique is becoming mature technique, however its thermo-mechanical behavior still need to be investigated and certain bench marking of tool design, reinforcements deposition strategy and process parameters is needed in order to replicate defect free hybrid composite materials mass production. There are many opportunities for developing hybrid composites using FSP on various Al alloys which are not yet exploited with huge possible combinations of variety of reinforcement particles from synthetic ceramic, industrial wastes, agricultural wastes and other possible metallic/nonmetallic materials.

REFERENCES

[1] R. Rajan, P. Kah, B. Mvola, J. Martikainen, Rev. Adv. Mater. Sci. **44**, 383-397 (2016).

[2] N.Z. Khan, A.N. Siddiquee, Z.A. Khan, A.K. Mukhopadhyay, J. Alloy. Compd. **695**, 2902-2908 (2017), DOI 10.1016/j.jallcom.2016.11.389.

[3] G. Mathers, The welding of aluminium and its alloys, 2002 Woodhead Publishing Limited, England.

[4] N.R. Mandal, Aluminium welding, 2002 Woodhead Publishing Limited and Alpha Science International Limited, England.

[5] H. Dong, Surface engineering of light alloys aluminium, magnesium and titanium alloys, 2010 Wood head Publications, England.

[6] A. Evans, C.S. Marchi, A. Mortensen, Metal Matrix Composites in Industry: An Introduction and a Survey, 2003 Springer Science Business Media, New York, DOI 10.1007/978-1-4615-0405-4.

[7] M.O. Bodunrin, K.K. Alaneme, L.H. Chown, J. Mater. Res. Technol. **4**, 434-445 (2015), DOI: https://doi.org/10.1016/j.jmrt.2015.05.003.

[8] S. Rathee, S. Maheshwari, A.N. Siddiquee, Mater. Manuf. Process. **33**, 239-261 (2017), DOI: 10.1080/10426914.2017.1303162.

[9] M. Gui, S.B. Kang, K. Euh, Metall. Mater. Trans. A **36**, 2471 (2005).

[10] S.R. Bakshi, V. Singh, K. Balani, D.G. Mccartney, S. seal, A. Agarwal, Surf. Coat. Tech. **202**, 5162-5169 (2008), DOI: https://doi.org/10.1016/j.surfcoat.2008.05.042.

[11] C. Hu, H. Xin, T. N. Baker, Mater. Sci. Tech. Ser. **12**, 227-232 (1996).

[12] D. Pantelis, A. Tissandier, P. Manolatos, P. Ponthiaux, Mater. Sci. Tech. Ser. **11**, 299-303 (1995), DOI: https://doi.org/10.1179/mst.1995.11.3.299.

[13] C. Hu, T.N. Baker, J. Mater. Sci. **30**, 5047-5051 (1997), DOI: https://doi.org/10.1023/A:1018653030270.

[14] L.R. Katipelli, N.B. Dahotre, Mater. Sci. Tech. **17**, 1061-1068 (2001), DOI: https://doi.org/10.1179/026708301101511185.

[15] Y. Wang, X. Zhang, G. Zeng, F. Li, Compos. Part A-Appl. S. **32**, 281-286 (2001), DOI: https://doi.org/10.1016/S1359-835X(00)00118-4.

[16] Y. Wang, X. Zhang, G. Zeng, F. Li, Mater. Des. **21**, 447-452 (2000), DOI: https://doi.org/10.1016/S0261-3069(00)00036-4.

[17] S.H. Choo, S. Lee, S.J. Kwon, Metall. Mater. Trans. A **30**, 3131-3141 (1999), DOI: https://doi.org/10.1007/s11661-999-0224-4.

[18] R.S. Mishra, M.W. Mahoney, S.X. McFadden, N.A. Mara, A.K. Mukherjee, Scripta Mater. **42**, 163-168 (1999), DOI: https://doi.org/10.1016/S1359-6462(99)00329-2.

[19] R.S. Mishra, Z.Y. Ma, I. Charit, Mater. Sci. Eng. A **341**, 307-310 (2003).

[20] W.M. Thomas, E.D. Nicholas, J.C. Needham, M.G. Murch, P.T. smith, C.J. Dawes, Friction stir butt welding: GB Patent, 9125978.8, 1991-12-06.

[21] M.S. Weglowski, S. Dymek, C.B. Hamilton, Bulletin of the Polish Academy of Sciences: Technical Sciences **61**, 893-904 (2013), DOI: 10.2478/Bpasts-2013-0096.

[22] M.S. Weglowski, Advances in Manufacturing Science and Technology **37**, 2013, DOI: 10.2478/amst-2013-0023.

[23] M.S. Weglowski, Arch. Mech. Eng. **61**, 2014, DOI: 10.2478/meceng-2014-0031.

[24] M.S. Weglowski, A. Pietras, Arch. Metall. Mater. **56**, (2011), DOI: 10.2478/V10172-011-0086-9.

[25] R.A.O.A. Shailesh, Y. Naik, Arch. Metall. Mater. **63**, 203-210 (2018), DOI: 10.24425/118929.

[26] A. Yazdipour, M.A. Shafiei, K. Dehghani, Mater. Sci. Eng. A **527**, 192-197 (2009), DOI: https://doi.org/10.1016/j.msea.2009.08.040.

[27] N. Gangil, A.N. Siddiquee, S. Maheshwari, J. Alloys Compd. **715**, 91-104 (2017), DOI: https://doi.org/10.1016/j.jallcom.2017.04.309.

[28] N. Gangil, A.N. Siddiquee, S. Maheshwari, A.M.A. Ahmari, M.H. Abidi, Arch. Metall. Mater. **63**, 719-738 (2018), DOI: 10.24425/122398.

[29] J. Iwaszko, K. Kudła, K. Fila, Bulletin of the Polish Academy of Sciences: Technical Sciences **66**, 713-719 (2018), DOI: 10.24425/125338.

[30] Y. Huang, T. Wang, W. Guo, L. Wan, L.V. Shixiong, Mater. Des. **59**, 274-278 (2014), DOI: http://dx.doi.org/10.1016/j.matdes.2014.02.067.

[31] I. Polmear, D.S. John, J.F. Nie, M. Qian, Light Alloys: Metallurgy of the Light Metals, 2017 Academic Press Elsevier, Butterworth-Heinemann.

[32] G.A. Roeen, S.F.K. Bozorg, M. Nosko, S. Nagy, I. Matko, J. Mater. Eng. Perform. **27**, 471-482 (2018), DOI: https://doi.org/10.1007/s11665-018-3170-8.

[33] S. Singh, Keerti, K. Pal, J. Alloys Compd. **740**, 436-445 (2018), DOI:10.1016/j.jallcom.2017.12.069.

[34] R. Beygi, M.Z. Mehrizi, G.B. Eisaabadi, J. Mater. Eng. Perform. **26**, 1455-1462 (2017), DOI: 10.1007/s11665-017-2552-7.

[35] G. Azimiroeen, S.F.K. Bozorg, M. Nosko, L. Orovcik, J. Microsc. **270**, 3-6 (2018), DOI: 10.1111/jmi.12642.

[36] E.R.I. Mahmoud, M. Takahashi, T. Shibayanagi, K. Ikeuchi, Wear **268**, 1111-1121 (2010), DOI:10.1016/j.wear.2010.01.005.

[37] S. Dixit, A. Mahata, D.R. Mahapatra, S.V. Kailas, K. Chattopadhyay, Compos. B **136**, 63-71 (2018), DOI: 10.1016/j.compositesb.2017.10.028.

[38] S. Toros, F. Ozturk, I. Kacar, J. Mater. Process. Tech. **207**, 1-12 (2008), DOI: 10.1016/j.jmatprotec.2008.03.057.

[39] E.M. Zayed, N.S.M. El-Tayeb, M.M.Z. Ahmed, R.M. Rashad, Development and Characterization of AA5083 Reinforced with SiC and Al2O3 Particles by Friction Stir Processing, in: A. Ochsner, H. Altenbach (Eds.), Engineering Design Applications: Advanced Structured Materials 2019, Springer 2019, DOI: https://doi.org/10.1007/978-3-319-79005-3_2.

[40] K. Mahmood, R. Abdul, A. Taha, S. Muhammad, N. Kashif, S. Tayyab, J. Mater. Process Tech. **253**, 72-85 (2018), DOI: https://doi.org/10.1016/j.jmatprotec.2017.11.002.

[41] A. Heidarpour, S. Ahmadifard, S. Kazemi, Prot. Met. Phys. Chem. **54**, 409-415 (2018). DOI: 10.1134/S2070205118030279.

[42] M. Amra, K. Ranjbar, S.A. Hosseini, T. Nonferr. Metal Soc. **28**, 866-878 (2018), DOI: 10.1016/S1003-6326(18)64720-X.

[43] N. Yuvaraj, S. Aravindan, Vipin, T. Indian I. Metals **70**, 1111-1129 (2016), DOI: 10.1007/s12666-016-0905-9.

[44] P. Sahandi, F. Khodabakhshi, A. Simchi, A.H. Kokabi, Int. J. Fatigue **87**, 266-278 (2016), DOI: http://dx.doi.org/10.1016/j.ijfatigue.2016.02.007.

[45] F. Khodabakhshi, A.P. Gerlich, A. Simchi, A.H. Kokabi, Mater. Sci. Eng. A **626**, 458-466 (2015), DOI: https://doi.org/10.1016/j.msea.2014.12.110.

[46] S.A. Hossieni, K. Ranjbar, R. Dehmolaei, A.R. Amirani, J. Alloys Compd. **622**, 725-733 (2014), DOI: https://doi.org/10.1016/j.jallcom.2014.10.158.

[47] M. Amra, K. Ranjbar, R. Dehmolaei, J. Mater. Eng. Perform. **24**, 3169-3179 (2015), DOI: 10.1007/s11665-015-1596-9.

[48] A. Mostafapour, S.T. Khandani, Mater. Sci. Eng. A **559**, 549-557 (2013), DOI: http://dx.doi.org/10.1016/j.msea.2012.08.140.

[49] S. Soleymani, A. Abdollah-zadeh, S.A. Alidokht, Wear **278-279**, 41-47 (2012), DOI: 10.1016/j.wear.2012.01.009.

[50] H.I. Kurt, Compos. B. Eng. **93**, 26-34 (2016), DOI: 10.1016/j.compositesb.2016.02.056.

[51] S. Ahmadifard, S. Kazemi, A. Heidarpour, P. I. Mech. Eng. L.-J. Mat. **232**, (2015), DOI: 10.1177/1464420715623977.

[52] A. Sharma, V.M. Sharma, B. Sahoo, J. Joseph, J. Paul, J. Compos. Sci. **2**, 32-49 (2018), DOI: 10.3390/jcs2020032.

[53] V.M. Khojastehnezhad, H.H. Pouras, R.V. Barenji, P.I. Mech. Eng. L.-J. Mat. **233**, (2019), DOI: 10.1177/1464420717715048.

[54] R. Palanivel, I. Dinaharan, R.F. Laubscher, J.P. Davim, Mater. Des. **106**, 195-204 (2016), DOI: http://dx.doi.org/10.1016/j.matdes.2016.05.127.

[55] M. Narimani, B. Lotfi, Z. Sadeghian, Surf. Coat. Tech. **285**, 1-10 (2016), DOI: http://dx.doi.org/10.1016/j.surfcoat.2015.11.015.

[56] R.V. Barenji, V.M. Khojastehnezhad, H.H. Pouras, A. Rabiezadeh, J. Compos. Mater. **50**, 1457-1466 (2016), DOI: 10.1177/0021998315592007.

[57] T. Prakash, S. Sivasankaran, P. Sasikumar, Arab Journal of Science and Engineering **40**, 559-569 (2015), DOI 10.1007/s13369-014-1518-4.

[58] M. Kolli, D. Aruri, IMECE2013-64161 in: Proceedings of the ASME 2013 International Mechanical Engineering Congress and Exposition IMECE2013 November 15-21, 2013, San Diego, California, USA.

[59] A. Devaraju, A. Kumar, A. Kumaraswamy, B. Kotiveerachari, Mater. Des. **51**, 331-341 (2013), DOI:10.1016/j.matdes.2013.04.029.

[60] S.R. Anvari, F. Karimzadeh, M.H. Enayati, Wear **304**, 144-151 (2013), DOI: https://doi.org/10.1016/j.wear.2013.03.014.

[61] C.M. Rejil, I. Dinaharan, S.J. Vijay, N. Murugan, Mat. Sci. Eng. A **552**, 336-344 (2012), DOI: http://dx.doi.org/10.1016/j.msea.2012.05.049.

[62] M. Mansumi, F.M. Sani, S.F.K. Bozorg, H.R.Z. Rajani, Journal of Materials Science and Engineering with Advanced Technology **6**, 29-45 (2012).

[63] A. Kumar, A. Devaraju, B. Kotiveerachari, IMECE2013-64734 in: Proceedings of the ASME 2013 International Mechanical Engineering Congress and Exposition IMECE2013 November 15-21, 2013, San Diego, California, USA.

[64] N. Pol, G. Verma, R. Pandey, T. Shanmugasundaram, Def. Technol. **15**, 363-368 (2018), DOI: https://doi.org/10.1016/j.dt.2018.08.002.

[65] H.T. Naeem, M.J.E.T. **4**, 56-65 (2016), DOI: 10.18081/mjet/2016-4/56-65.

[66] I. Sudhakar, V. Madhu, G.M. Reddy, K.S. Rao, Def. Technol. **11**, 10-17 (2015), DOI: http://dx.doi.org/10.1016/j.dt.2014.08.003.

[67] S. Mahmoud, K.B.S. Farshid, H. Alimohamad, Advanced Processes in Materials **10**, 47-57 (2016), https://www.sid.ir/en/journal/ViewPaper.aspx?ID=519496.

[68] A. Mina, S. Morteza, G. M. Ali, Iranian Journal of Surface Science and Engineering **12**, 41-51 (2017), https://www.sid.ir/en/journal/ViewPaper.aspx?ID=570877.

[69] M. Akbari, P. Asadi, P. Zolghadr, A. Khalkhali, P. I. Mech. Eng. E.-J. Pro. **232**, 323-337 (2017), DOI: 10.1177/0954408917704994.

[70] S.A. Alidokht, A. Abdollah-zadeh, S. Soleymani, H. Assadi, Mater. Des. **32**, 2727-2733 (2011), DOI: 10.1016/j.matdes.2011.01.021.

[71] P. Gurusamy, A.J. Pandian, L.C. Bestall, IJVSS **7**, 175-178 (2015), DOI: 10.4273/ijvss.7.4.13.

[72] M. Janbozorgi, M. Shamanian, M. Sadeghian, P. Sepehrinia, T. Nonferr. Metal. Soc. **27**, 298-304 (2017), DOI: 10.1016/S1003-6326(17)60034-7.